Study of Flexible Wheels for Lunar Exploration Rovers: Running Performance of Flexible Wheels with Various Amount of Deflection

Kojiro Iizuka [1] and Takashi Kubota [2]

[1] *International Yong Researchers Empowerment Center, Shinshu University, iizuka@shinshu-u.ac.jp*
[2] *Japan Aerospace Exploration Agency, kubota@isas.jaxa.jp*

Abstract

Lunar rovers are required to traverse rough terrains with craters and sheer cliffs—often seen in locations of scientific importance. Recently, wheeled rovers have been gaining popularity in conducting planetary exploration missions. However, wheeled rovers are likely to get stuck in the soil while traversing such terrains. One way to solve this problem is to use flexible wheels. In this study, experiments were carried out to simulate actual running conditions using flexible wheels. The results showed that flexible wheels had a high level of performance when traversing loose soil on a slope. The experiments were carried out using various flexible wheels that allowed different amounts of deflection. The flexible wheels were made from beryllium copper, magnesium, and stainless steel. In these experiments, we measured slip ratio and sinkage for each of these materials.

Keywords

lunar rover, flexible wheel, loose soil, elastic, terra mechanics

1. INTRODUCTION

Robots are considered one of the most important mission devices for planetary exploration; they are expected to traverse planetary surfaces to collect precise information regarding the origin and maturity. The NASA Mars mission in 1997 was accomplished using the micro robot Sojourner that traversed and explored the surface of Mars. Sojourner transmitted important data and detailed pictures to the earth. The Sojourner mission showed the importance of roving exploration [NASA/JPL, 1997]. In planetary explorations, robots are required to traverse rough terrains that include craters and sheer cliffs, which are locations of scientific importance that need to be explored. Further, while traversing such terrains, robots should not tip over and get stuck in the soil.

As a matter of fact, MER [NASA/JPL] got stuck while traversing loose soil. In this study we have carried out experiments simulating actual running conditions using a circular rigid wheel similar to the ones currently used in rovers. When a circular rigid wheel traverses loose soil concomitant with slope, the slip behavior of the wheel becomes pronounced. If slip behavior of the wheel increases, the wheel is liable to sink. Therefore, it can be concluded that a circular rigid wheel can't traverse rough terrains that include craters and sheer cliffs. This is because the running performance of the circular wheel decreases when it traverses on loose soil, owing to, what we believe, is its tendency to sink. We need to produce a wheel without the tendency to sink. Therefore, in this paper we propose the use of a wheel using flexible material [Iizuka et al, 2008] (Figure 1). The proposed flexible wheel can give bet-

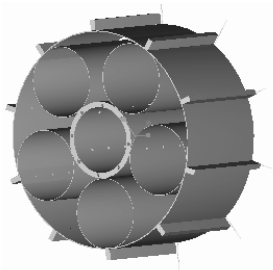

Fig. 1 Proposed Flexible Wheel [Iizuka, 2008]

(a) Tweel [NASA/Mishelin]

(b) ExoMars [ESA]

Fig. 2 Flexible wheel

ter performance than a circular rigid wheel. When a flexible wheel comes in contact with the ground, the bottom of the wheel changes in shape to match the contours of the surface of the ground. Therefore, the flexible wheel does not show a tendency to sink because the stress of the flexible wheel is low. For these very reasons, NASA and ESA have independently developed flexible wheels, too (Figure 1). NASA/Michelin developed a flexible wheel using compound material. On the other hand, ESA developed a flexible wheel using stainless steel. In addition, ESA has considered using a ribbed design.

In these designs, no doubt the contact area of the flexible wheel with the ground increases; however, little consideration has been given to the amount of deflection of the flexible wheel. Therefore, this paper considers this aspect experimentally.

In section 2, the interaction between flexible wheels and loose soil is modeled. In section 3, the experiment and its results are described. In section 4, the conclusions of this study are provided.

2. INTERACTION MODEL BETWEEN FLEXIBLE WHEEL AND LOOSE SOIL

In this study, the interaction between a circular rigid wheel in motion and loose soil was examined [Iizuka et al., 2005]. From the experimental results, we obtained the clarification that the poor running condition of the wheel can be attributed to its tendency to sink.

We then go on to describe an interaction model between a flexible wheel and loose soil. Over the past few years, several studies have been conducted on an interaction model for a circular solid wheel [Bekker, 1955] [Yon et al., 1986] [Yoshida et al., 2001] [Iagnemma et al., 2002] [Ishigami et al., 2006]. Moreover, Muro [Muro, 1993] has modeled the interaction between low-stress tires and the ground. The wheels that are to be used on the lunar surface must be made of metal in order to withstand the unique environment on the lunar surface that includes vacuum conditions, radioactive rays, and large variations in temperature.

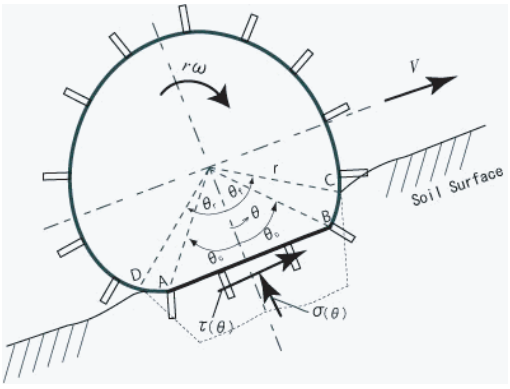

Fig. 3 Interaction model

A flexible wheel made of metal can change its form. The material used on the surface of a flexible wheel is spring steel. When a wheel made using spring steel is loaded with weight, its form changes such that the part of the wheel that is in contact with the ground becomes flat. The interaction model between a flexible wheel and loose soil is shown in Figure 3.

The surface of the flexible wheel becomes flat on the surface of the ground. Traction force is an important factor that must be considered during traversal on the ground. In this study, we propose an advanced model. This model is based on that developed by Muro. However, Muro's model does not consider the effect of the lugs on the wheels.

Therefore, in this study, we propose an advanced model that includes the effect of the lugs (Figure 4). The traction force DP is determined using various parameters such as the radius of the wheel, r; the entry angle, θ_f; the exit angle, θc; the normal stress, $\sigma(\theta)$; the shear stress, $\tau(\theta)$; the length of the flat side between the points A and B, l_{AB}; the reaction stress, R_b; the length of the lugs, L_j; the width of the wheel, b; and the slip ratio, λ.

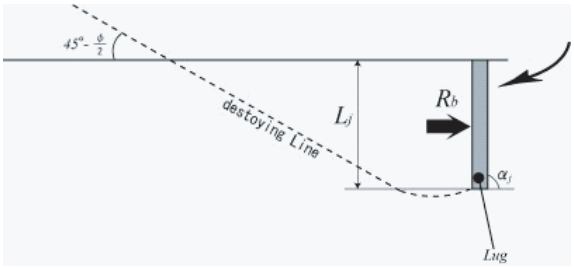

Fig. 4 Model of a lug

When the lugs sink into the soil, the wheel experiences a reaction stress from the soil. The reaction stress is expressed using L_j as follows:

$$DP = rb\left\{\int_{\theta c}^{\theta_f} Ad\theta + \frac{1}{r}\int_0^{l_{AB}} \tau(\theta)d\theta + \int_{\theta r}^{\theta_c} Ad\theta\right\} + L_j by\left\{\int_{\theta c}^{\theta_f} Bd\theta + \int_{\theta c}^{\theta_f} B\frac{1}{\cos\theta}d\theta + \int_{\theta r}^{\theta_c} Bd\theta\right\} \quad (1)$$

where

$$A = \tau(\theta)\cos\theta - \sigma(\theta)\sin\theta$$
$$B = R_b\cos\theta$$
$$R_b = \frac{\sin(\alpha_j + \phi)}{\sin\alpha_j}\left\{L_j c(N_c - \tan\phi) + \frac{1}{2}\gamma L_j^2\left(\frac{2N_r}{\tan\phi} + 1\right)\right. \quad (2)$$

where

α_j: angle of approach
γ: soil density

L_j: lug length
c: cohesion stress
ϕ: friction angle of soil
N_c, N_r: coefficients of support force

As observed in Figure 3, in this model, it is important to consider the flat part of the wheel, i.e., the part between points A and B. In this flat part, the reaction force applied by the soil to the wheel and also the lugs is significant. Therefore, it is important to capture the amount of deflection. This paper measures running performance with various amounts of deflection.

3. EXPERIMENT STUDY

3.1 Experiment system

The overview of the experimental system is shown in Figure 5. Figure 6 shows a photograph of the experimental system. In this experiment, the simulant was soil, having a particle specific gravity of 2.83, a minimum density of 1.39 [g/cm^3], an adhesive power of 5.0 [kPa], and an internal friction angle of 36.7 [°]. The thickness of the loose soil was 0.07 [m]. It was dried using a heater. The experimental system comprised some mechanical parts and sensors, as shown in Figure 5. A single wheel, a parallel link, stator, guide rail, load balance, and balance box were used for carrying out the simulation. The parallel link was attached between the axis of the wheel and the load balance. The load balance ran on the guide rail. The sensors included a differential transformer and two encoders. The differential transformer was used to measure the horizontal position of the wheel. The maximum distance measurable by the differential transformer is 20 mm. The vertical position of the wheel was calculated using a rotary encoder. The velocity of the wheel was calculated by using the vertical and horizontal positions and the time taken by the wheel to cover a certain distance. The rotation of the wheel was obtained from the encoder. The slip ratio was calculated using the values of velocity and rotation. Sinkage was determined by measuring the depth of the soil before and after performing the running experiments, and estimating the difference. The load on the wheel was set by placing an appropriate weight in the balance box.
In the parameters experiment, the load on the wheel and the angle of the slope could be varied. The experimental parameters are listed in Table 1.

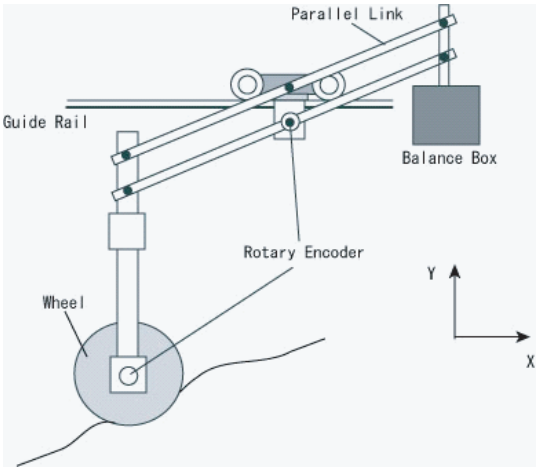

Fig. 5 Experiment system

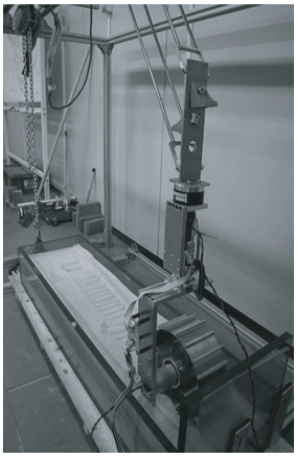

Fig. 6 View of experiment systems

Table 1 Experimental parameters

	Value	Unit
Load	3.0, 4,5, 6	kg
Speed	0.1	m/s
Slope	15, 20, 25	°

3.2 Flexible wheels for experiments

Figure 7 shows the wheels used for the experiments. This study has used a circular rigid wheel too (Figure 7 (a)). There are three types of flexible wheels (Figure 7 (b)), beryllium copper (Young ratio: GPa) wheel, magnesium (Young ratio: GPa) wheel and stainless steel (Young ratio: GPa) wheel.

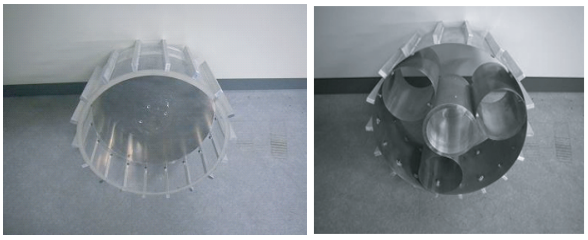

(a) Circular rigid wheel (b) Flexible wheel

Fig. 7 Wheels for experiment

3.3 Deflection of flexible wheels

Table 2 shows the deflection of the different types of

Table 2 Deflection of flexible wheels

	Deflection [mm]		
Load [kg]	3	4.5	6
Circular Rigid	0	0	0
Beryllium Cop.	12.51	20.80	26.98
Magnesium	6.27	12.51	18.73
Stainless Steel	0.00	4.18	18.73

flexible wheels with various loads (3, 4.5, and 6 kg). The deflection of the wheel made from beryllium copper is largest amongst all wheels. The stainless steel flexible wheel shows no change at 3 kg. Moreover, when the magnesium flexible wheel is set a 6 kg load, its deflection is the same as that of stainless steel wheel. This means that the limit of deflection of magnesium is small when compared to that of beryllium copper and stainless steel. In these experiments, we have captured the running performance using these wheels.

3.4 Results

Figure 8 shows the result of the experiments in which actual running conditions were simulated. Figure.8 (a) is the result at 3.0 kg, (b) is at 4.5 kg, and (c) is at 6.0 kg. When the load on the wheel increases, the slip ratio of the all wheels becomes large. At a load of 3 kg, the slip ratios of all the wheels are the same. When the load on the wheel becomes 4.5 kg, the slip ratios become divergent. Notably,when the load on the wheel is 3.5 kg, the slip ratios of Magnesium and Beryllium copper wheels are smaller than that of the other two wheels. Moreover, at 6 kg, the slip ratio of Beryllium copper wheel is the smallest of all the wheels.

Figure 9 shows the results of the experiments at various slopes ((a) 15, (b) 20, (c) 25 kg). When the wheels traverse on slope 15°, wheels made from beryllium copper and magnesium are more effective compared to other wheels. Moreover, if the slope is 20 and 25°, slip ratios of all wheels come close to a same value. As per these results, when the slip ratios are larger than around 0.5, all the wheels have the same running performance.

Figure 10 shows sinkage of the wheels at various loads and slopes. When the slope becomes large, the sinkages of the wheels are large. Moreover, all wheels show the same sinkage when the slope becomes large. Therefore, there isn't a large change even when the form of the wheel changes.

Figure 11 shows the slip ratio for all Young's moduli that each wheel has and plots the value of the maximum and minimum. On each slope, Young's modulus with the beryllium copper wheel is effective. Moreover, when the wheel has a 6.0 kg load, Young's modulus with beryllium copper wheel is very effective.

Figure 12 shows the slip ratio for each deflection. When the slope becomes large, deflections of each wheel become large. If the slope is 15 or 20°, the slip ratio on the wheel with 3 kg load shows a tendency to become large. However, when the wheel has a load of 4.5 or 6 kg at 15 and 20°, the slip ratio displays a tendency to become lower with increase in load.

4. DISCUSSION

This paper describes the running performance of flexible wheels with various deflections. The quantum of deflection that we set varied from 0 mm to 26.98 mm. In addition, we carried out experiments on loose soil with three kinds of slope (15, 20, 25°). In general, when the slope increases, the slip ratio increases. Sinkage also increases similar to the tendency of the slip ratio. Further, when the slope is over 25°, the running performances of the various types of wheels is not different. We think that the limit of the slope is around 25°, in the case of the flexible wheels used in

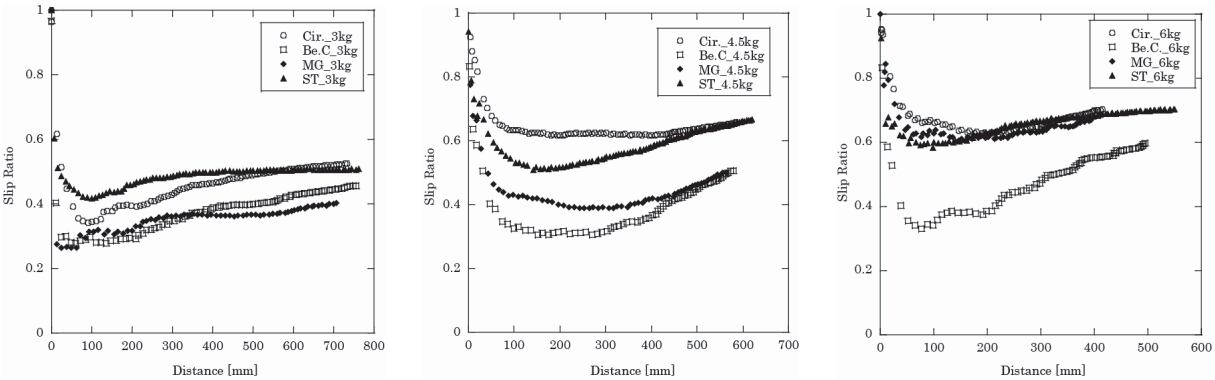

(a) 3.0 kg (b) 4.5 kg (c) 6.0 kg

Fig. 8 Experiment result of slip ratio (15 [°])

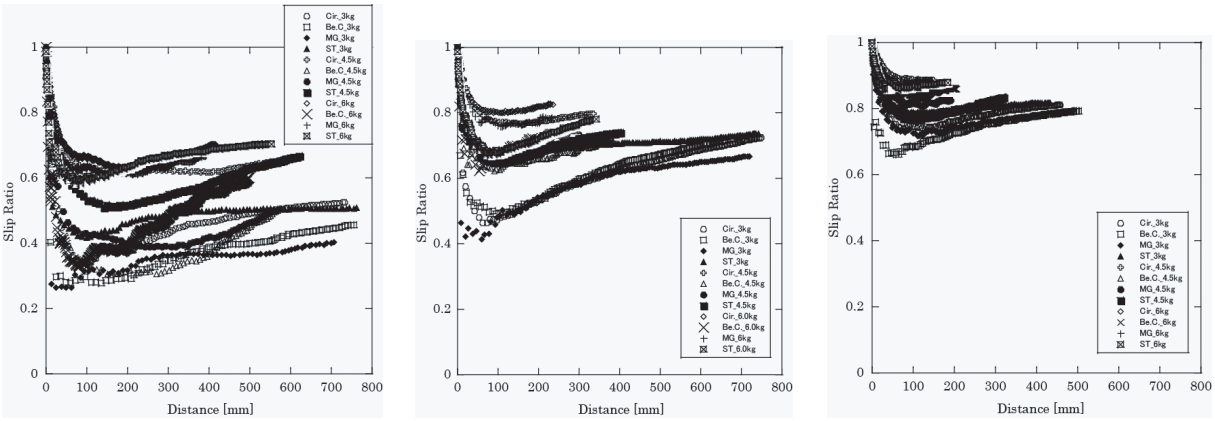

(a) 15° (b) 20° (c) 25°

Fig. 9 Experiment result of slip ratio (15, 20, 25°)

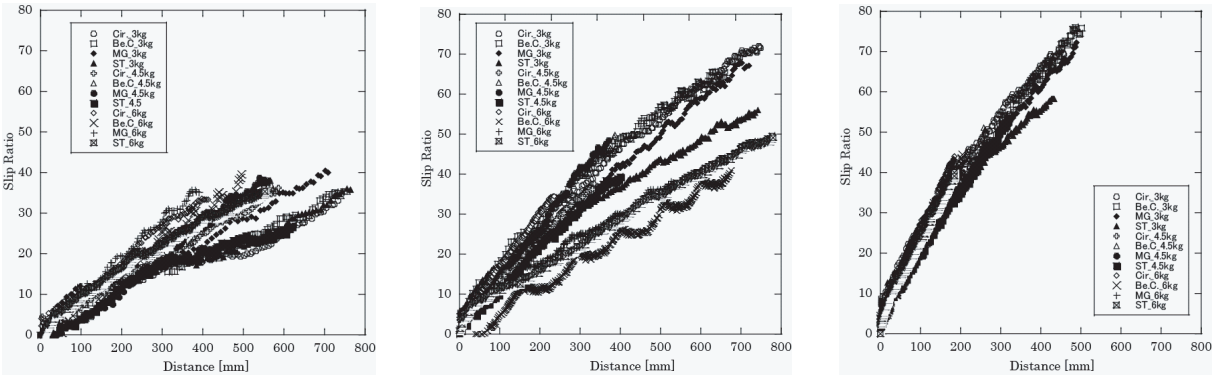

(a) 15° (b) 20° (c) 25°

Fig. 10 Experiment result of sinkage (15, 20, 25°)

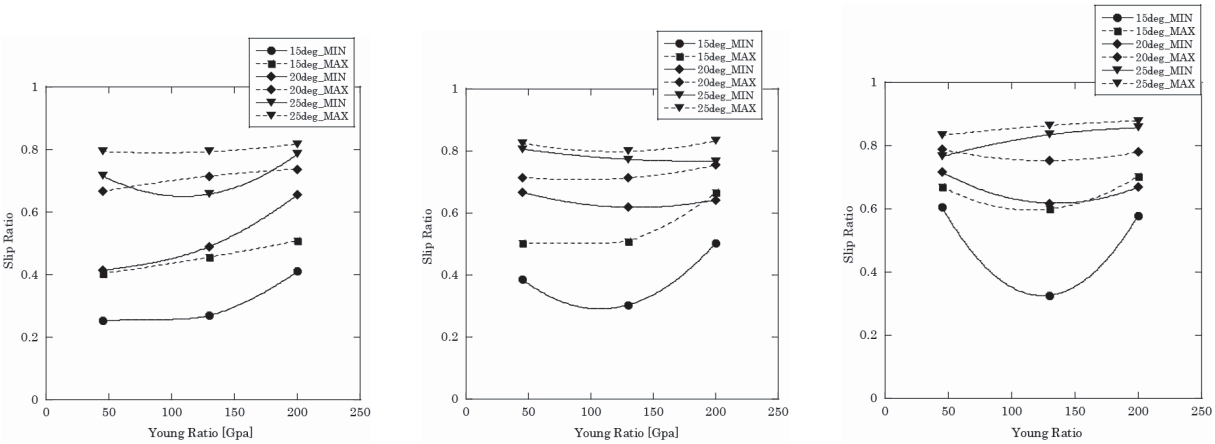

(a) 3.0 kg (b) 4.5 kg (c) 6.0 kg

Fig. 11 Experiment result of slip ratio (For various Young's moduli)

our study. However, when the load on the wheels is at 3 kg, if the deflection becomes large i.e., 25°, the slip ratio shows a tendency to go down. We believe that the slip ratio can be decreased if the deflection of the wheel with 3 kg weight is over 15 mm at 25° slope. Therefore, this study demonstrates that the flexible wheel has a possibility to traverse loose soil with 25° slope through the device of increasing deflections of the wheel.

5. CONCLUSION

In this paper, we have described a wheel that can be used in lunar rovers. We have measured the running performance using wheels with various materials, as

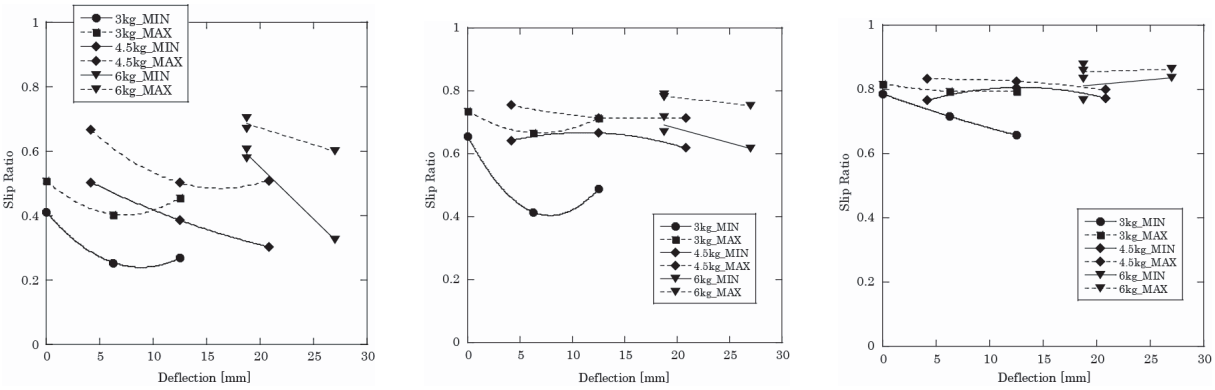

(a) 15° (b) 20° (c) 25°

Fig. 12 Experiment result of slip ratio (for various deflections)

well as the deflection and Young's modulus. In the future, we will be determining the optimal elastic force by carrying out simulation and experiments using flexible wheels with larger deflection.

Acknowledgement

This study was partly supported by Special Coordination Funds for Promoting Science and Technology for Young Researcher Empowerment Project from the Ministry of Education, Culture, Sports, Science and Technology (MEXT), Japan.

References

Bekker, M., *Theory of land locomotion*, The University of Michigan Press, 1955.

Iagnemma, K., H. Shibly, and S. Dubowsky, On-line terrain parameter estimation for planetary rovers, *2002 IEEE International Conference on Robotics and Automation*, 3142-3147, 2002.

Iizuka, K., Y. Kunii, and T. Kubota, Study on wheeled forms of lunar robots considering flexible characteristic of traversing loose terrain, *Transactions of the Japanese Society of Mechanical Engineers*, Vol.74, No.748, 2962-2967, 2008.

Ishigami, G., K. Nagatani, and K. Yoshida, Path following control with slip compensation on loose soil for exploration rover, *Proceedings of 2006 IEEE/RSJ International Conference on Intelligent Robots and Systems*, 5552-5557, 2006.

Muro, T., *Terramechanics: Running dynamics*, Gihodo Press, 1993.

NASA/JPL, http://mars.jpl.nasa.gov/MPF/Sojourner.html, 2009.

NASA/JPL, http://marsrovers.jpl.nasa.gov/home/, 2009.

Yoshida, K., and H. Hamano, Motion dynamics simulations and experiments of an exploration rover on natural terrain, *Astrodynamics and Flight Mechanics*, No.11, 306-313, 2001.

Yon, R. N., E. Fattah, N. Skidas, and M. Kitano, *Run dynamics of off-road vehicles*, The Japanese Society for Study Technology Education, 1986.

(Received November 16, 2009; accepted December 9, 2009)